

Variational study of the Holstein polaron

O. S. Barišić*

Institute of Physics, Bijenička c. 46, HR-10000 Zagreb, Croatia

(Received 10 January 2001; revised manuscript received 24 May 2001; published 12 March 2002)

The paper deals with the ground and the first excited state of the polaron in the one-dimensional Holstein model. Various variational methods are used to investigate both the weak-coupling and strong-coupling case, as well as the crossover regime between them. Two of the methods, presented here, introduce interesting elements to the understanding of the nature of the polaron. Reliable numerical evidence is found that, in the strong-coupling regime, the ground and the first excited state of the self-trapped polaron are well described within the adiabatic limit. The lattice vibration modes associated with the self-trapped polarons are analyzed in detail, and the frequency softening of the vibration mode at the central site of the small polaron is estimated. It is shown that the first excited state of the system in the strong-coupling regime corresponds to the excitation of the soft phonon mode within the polaron. In the crossover regime, the ground and the first excited state of the system can be approximated by the anticrossing of the self-trapped and the delocalized polaron state. In this way, the connection between the behavior of the ground and the first excited state is qualitatively explained.

DOI: 10.1103/PhysRevB.65.144301

PACS number(s): 71.38.-k, 63.20.Kr

I. INTRODUCTION

Ever since Landau¹ suggested that the electron can be trapped by the deformable lattice, strongly coupled electron-phonon systems have been the subject of intensive examination. Besides the investigations of those systems in which the lattice is coupled to the whole electronic band, there has been significant interest in the physics of a single polaron, in which the electron and the associated lattice deformation form a quasiparticle, spatially and spectrally decoupled from the rest of the system. Lattice degrees of freedom make even a single polaron problem a many-body one. The analytical and numerical examinations of most electron-phonon models are thus difficult. For this reason, even the simple Holstein model² (suggested in 1959) is still being investigated in recent works. Various methods have been proposed in order to calculate the polaron ground state of the Holstein model. Almost exact results (except for the adiabatic limit) have been obtained with the quantum Monte Carlo calculations,^{3,4} the global-local method,⁵ the density-matrix renormalization-group method,⁶ and some exact diagonalization methods.^{22,23}

The main goal of this paper is to determine the elements important for the qualitative description of the polarons in the whole range of electron-phonon coupling. Some of them, although already known, are found to be better understood when supplemented with additional details.

The ground state of the Holstein system changes from the delocalized polaron state, in which the electron is nearly free, to the small and self-trapped polaron state, as the electron-phonon coupling g increases. These two opposite limits are usually identified as the weak- and strong-coupling regime, respectively. In the weak-coupling regime the influence of the small lattice deformation on polaron dynamics is very small, which makes the energies of polaron and electron hopping to neighboring sites similar, $t_{pol} \lesssim t$.

The exact ground state is an eigenstate of the system momentum, regardless of the coupling.⁷ Therefore the polaron ground state is delocalized for all parameters. However, in the strong-coupling regime t_{pol} becomes negligible, leading

to *self-trapped* polaron states. According to Ref. 8, the dynamics of the small self-trapped polaron can be separated into two time scales. On the short time scale, the lattice deformation is centered at some lattice site, and the electron can virtually hop among the neighboring lattice sites. Only after a certain number of such events (of the order t_{pol}/t), the polaron as a whole tunnels to a new central site. The localized polaron states thus may lead to a very accurate estimation of the polaron ground-state energy in the strong coupling regime. Accordingly, for the self-trapped polarons, an exact diagonalization method of calculating the localized polaron states, rather than the translationally invariant ones, can be used. By comparison to the results of other methods, it is shown that this approach introduces only minor errors in the ground-state energy of the self-trapped polaron. Moreover, the localized polaron functions permit, unlike the translationally invariant ones, a separate analysis of the electron and phonon properties of the polaron. The local electron density, the mean lattice deformation, and the on-site zero point motions of the self-trapped polarons can be calculated in this way.

In the crossover (intermediate) regime, which is between the weak- and the strong-coupling regime, no known perturbation calculation converges, which complicates the discussion of the polaron nature. Although it has been proved that the change of the polaron ground state with g is smooth,⁹ the physics of the rapid crossover between two opposite limits of the electron-phonon coupling, in the small interval of g 's, is not completely clear. In Ref. 23 it has been claimed that the phonon excitation associated with the first excited state of the system is uncorrelated to the electron in the weak-coupling regime, while it is confined to the electron in the strong-coupling regime. The transition occurs in the crossover regime in which, in addition, the energy difference between the ground and excited states becomes small. In the present paper, the excited polaron states are treated by the method which uses variational approach in order to define and solve the generalized eigenvalue problem. Even if this method does not converge systematically, it does provide

interesting results concerning the nature of the polaron ground and first excited state.

II. GENERAL

The Holstein Hamiltonian reads

$$\hat{H} = -t \sum_{n,s} c_{n,s}^\dagger (c_{n+1,s} + c_{n-1,s}) + \hbar\omega \sum_n b_n^\dagger b_n - g \sum_{n,s} c_{n,s}^\dagger c_{n,s} (b_n^\dagger + b_n). \quad (1)$$

It describes the tight-binding electrons in the nearest-neighbor approximation, coupled to one branch of dispersionless optical phonons. $c_{n,s}^\dagger$ is the creation operator for the electron of spin s at lattice site n , and b_n^\dagger is the creation operator for the phonon. t is the transfer (hopping) integral of the electron. $\hbar\omega$ and g are the phonon and the electron-phonon coupling energies, respectively. The Holstein Hamiltonian depends only on two ratios of relevant energy parameters: $g/\hbar\omega$ and $t/\hbar\omega$, i.e., the results will use $\hbar\omega$ as the energy unit. It is often convenient to express the lattice vibrations in terms of the nuclei space and momentum coordinates,

$$\hat{x}_n = x_0 (b_n^\dagger + b_n), \quad \hat{p}_n = ip_0 (b_n^\dagger - b_n), \quad (2)$$

where $x_0 = \sqrt{\hbar/2M\omega}$ and $p_0 = \sqrt{M\hbar\omega/2}$ are space and momentum uncertainties of the harmonic oscillator ground state. M is the mass of a nucleus and κ denotes the spring constant, $\omega^2 = \kappa/M$. By noting that the electron-lattice displacement coupling constant α , in $g = \alpha x_0$, is independent of M , an alternative set of Holstein Hamiltonian parameters can be introduced,

$$t = \hbar^2/2m_{el}a^2, \quad M = \frac{\kappa}{\omega^2}, \quad \varepsilon_p = \frac{\alpha^2}{2\kappa} = \frac{g^2}{\hbar\omega},$$

which is convenient for the discussion of the adiabatic regime $M \gg m_{el}$. Here, m_{el} is the electron effective mass and a is the lattice constant. It is worth noting that t and ε_p (the binding energy of the polaron for $t=0$) are independent of M and thus they are the only parameters relevant in the adiabatic limit.

By using standard conventions for $c_{k,s}^\dagger$ and b_q^\dagger ,

$$c_{k,s}^\dagger = 1/\sqrt{N} \sum_n e^{-ikna} c_{n,s}^\dagger, \quad b_q^\dagger = 1/\sqrt{N} \sum_n e^{-iqna} b_n^\dagger,$$

Eq. (1) can be rewritten in momentum space and separated in two mutually commuting parts, $\hat{H} = \hat{H}_{k,q \neq 0} + \hat{H}_{q=0}$,

$$\hat{H}_{k,q \neq 0} = -2t \sum_{k,s} \cos(ka) \hat{n}_{k,s} + \hbar\omega \sum_{q \neq 0} \hat{n}_q - g/\sqrt{N} \sum_{k,s,q \neq 0} c_{k+q,s}^\dagger c_{k,s} (b_q + b_{-q}^\dagger),$$

$$\hat{H}_{q=0} = \hbar\omega \hat{n}_{q=0} - gN_{el}/\sqrt{N} (b_{q=0} + b_{q=0}^\dagger),$$

where $\hat{n}_{k,s} = c_{k,s}^\dagger c_{k,s}$, $\hat{n}_q = b_q^\dagger b_q$, and $N_{el} \equiv \sum_{k,s} \hat{n}_{k,s}$.

The part which involves only the $q=0$ phonon mode, $\hat{H}_{q=0}$, can easily be transformed into the diagonal form, by using the unitary operator $\hat{S}_q(\xi)$,

$$\hat{S}_q(\xi) = \exp(\xi b_q^\dagger - \xi^* b_q),$$

$$\hat{S}_{q=0}^{-1}(\xi) \hat{H}_{q=0} \hat{S}_{q=0}(\xi) = \hbar\omega \hat{n}_{q=0} - (N_{el}g)^2/N\hbar\omega,$$

where $\xi = N_{el}g/\sqrt{N}\hbar\omega$. Any eigenstate of $\hat{H}_{q=0}$, $\hat{S}_{q=0}(\xi)|n_{q=0}\rangle$, has the same mean total lattice deformation, $\bar{x}_{tot} = \sum_n \bar{x}_n$,

$$\begin{aligned} \bar{x}_{tot} &= x_0 \sqrt{N} \langle n_{q=0} | \hat{S}_{q=0}^{-1}(\xi) (b_{q=0}^\dagger + b_{q=0}) \hat{S}_{q=0}(\xi) | n_{q=0} \rangle \\ &= x_0 \sqrt{N} (\xi^* + \xi) = 2x_0 N_{el}g/\hbar\omega, \end{aligned} \quad (3)$$

which is independent of t . Since the $q=0$ part of the Hamiltonian commutes with $\hat{H}_{k,q \neq 0}$, it can be concluded that Eq. (3) is also valid for all eigenstates of the total Holstein Hamiltonian. The phonon part of these eigenstates can be represented in the form of a direct product of two groups of states, the first one includes $q \neq 0$ phonon modes, while the second includes only the $q=0$ phonon mode. This is useful because one can always check approximate computations by calculating \bar{x}_{tot} , or include this property in the computation itself. This specific property of the $q=0$ mode is not restricted to the particular dimension of the system, nor to the number of electrons. Moreover, it can also be found in some other models in which the electron-phonon coupling consists of the lattice deformation linearly coupled to the local electron density. A hint in this direction was reported in Ref. 10.

The total momentum of the system, \hat{K} , is the sum of the electron and phonon momenta,

$$\hat{K} = \sum_k k \hat{n}_k + \sum_q q \hat{n}_q,$$

and it commutes with the Hamiltonian. In the present treatment, only the low-energy polaron states (the low-lying states of the system for which the electron and lattice part of the wave function are spatially bound), are explicitly calculated. In this case, the total momentum K of the system is also the polaron momentum.

III. METHODS

The eigenstate computations reported here are based on the variational approach. Still, from the physical and mathematical point of view, there are significant differences among them. Each method is therefore described separately in the present section. It is important to notice that two qualitatively different kinds of polaron functions are employed, the *localized* ones and the *translationally invariant* ones. The primary objective of the methods with localized functions are self-trapped polaron states, i.e., the strong-coupling regime. On the other hand, translationally invariant states are

devised in the first place with the weak coupling and cross-over regime in mind. The methods with a small number of variational parameters are meant to help in understanding the basic properties of the polarons in different regimes of the Holstein model. Again, the methods with a very large number of variational parameters are necessary to obtain accurate results for the polaron states.

A. L method: A simple localized polaron function

Let us start with a simple localized polaron wave function formed as a product of the electron and the lattice part, centered at the lattice site j ,

$$|\varphi_j\rangle = \left(\sum_n \eta_n c_{j+n}^\dagger \right) \left(\prod_m S_{j+m}(\xi_m) \right) |0\rangle. \quad (4)$$

Here, η_n is the normalized electron function at site $j+n$, $\sum_n \eta_n^* \eta_n = 1$, while $S_{j+m}(\xi_m)$ denotes the coherent state operator acting on site $j+m$, with a complex amplitude, $\xi_m = \text{Re}(\xi_m) + i\text{Im}(\xi_m)$,

$$S_{j+m}(\xi_m) = \exp(\xi_m b_{j+m}^\dagger - \xi_m^* b_{j+m}).$$

It is easy to see that operator $S_{j+m}(\xi_m)$ shifts the space and momentum coordinates of lattice vibration at a site $j+m$ by $2 \text{Re}(\xi_m)x_0$ and $2 \text{Im}(\xi_m)p_0$, respectively,

$$S_{j+m}(\xi_m) = e^{[i2 \text{Im}(\xi_m)p_0 \hat{x}_{j+m}/\hbar]} e^{[-i2 \text{Re}(\xi_m)x_0 \hat{p}_{j+m}/\hbar]} \times e^{[i \text{Re}(\xi_m)\text{Im}(\xi_m)]}.$$

The variational energy of the state (4), \bar{E}_φ , is independent of j , and is given by

$$\begin{aligned} \bar{E}_\varphi = & -t \sum_n \eta_n^* (\eta_{n-1} + \eta_{n+1}) + \hbar\omega \sum_n |\xi_n|^2 \\ & - g \sum_n |\eta_n|^2 (\xi_n + \xi_n^*). \end{aligned} \quad (5)$$

The minimization of the energy with respect to ξ_n establishes a simple relationship between the lattice mean deformation and electron density $\varrho_n = |\eta_n|^2$,

$$\xi_n = (g/\hbar\omega)\varrho_n \Rightarrow \bar{x}_n = (\alpha/\kappa)\varrho_n, \quad (6)$$

so that only the equation for η_n has to be solved. The well-known approximate solution to this problem is the large Holstein polaron² valid in the long-wave limit,

$$\eta_n = \frac{1}{\sqrt{2d_{pol}}} \cosh^{-1}(n/d_{pol}), \quad d_{pol} = \frac{2t\hbar\omega}{g^2} = \frac{2t}{\varepsilon_p}. \quad (7)$$

The numerical scheme suggested in Ref. 11, and denoted here by L (L for localized), is not restricted to long waves, and is used here in order to obtain the exact minimum of Eq. (5). The energy, henceforth referred to as E_L , depends only on two relevant Hamiltonian parameters, t and $g^2/\hbar\omega = \varepsilon_p$, and therefore E_L and \bar{x}_m^L are both independent of M . For this reason Eq. (6) is sometimes referred to as the adiabatic locking of electron and lattice coordinates.

It is noteworthy that the lattice part of the function $|\varphi\rangle_j^L$ is a simple product of coherent states with real amplitudes. Consequently, the state of the lattice at some site is defined by the ground state of the displaced harmonic oscillator. The mean lattice deformation \bar{x}_m^L corresponds to the equilibrium position of that oscillator, while the lattice zero-point motion is approximated in Eq. (4) by that of the free lattice.

B. T and CT methods: Translational polaron functions and the first excited state

Next, we shall study a translationally invariant solution composed of a linear superposition of the localized states (4),

$$|\Psi_K\rangle = \frac{1}{\sqrt{N_\Psi}} \sum_j e^{iKja} |\varphi_j\rangle. \quad (8)$$

$|\Psi_K\rangle$ describes the polaron state with the momentum K . A similar type of function was proposed by Toyozawa.¹² In the present work, $\sum_m \xi_m = g/\hbar\omega$ is used so that the mean total deformation of function (8) satisfies Eq. (3),

$$\bar{x}_{tot} = x_0 \sum_m \langle \Psi_K | (b_m^\dagger + b_m) | \Psi_K \rangle = 2x_0 g/\hbar\omega.$$

The expectation value of the polaron energy, \bar{E}_Ψ , may be written in terms of $|\varphi_j\rangle$,

$$\bar{E}_\Psi = \frac{\sum_\Delta e^{iK\Delta a} \langle \varphi_j | \hat{H} | \varphi_{j+\Delta} \rangle \sum_\Delta e^{iK\Delta a} E_\Delta}{\sum_\Delta e^{iK\Delta a} \langle \varphi_j | \varphi_{j+\Delta} \rangle \sum_\Delta e^{iK\Delta a} S_\Delta}. \quad (9)$$

E_Δ and S_Δ are given in the Appendix. A simple method for calculating the minimum of the energy \bar{E}_Ψ has not yet been proposed, but accurate results have been obtained in Ref. 13 by using the Toyozawa method, which includes a very large number of variational parameters. Some additional approximations may be found in Refs. 10 and 14–18. The approximation used here simplifies the general expression in Eq. (8) by introducing the exponential form for functions η_n and ξ_m ,¹⁶

$$\eta_n = CG^{|n|}, \quad \xi_m = AB^{|m|} e^{iKma}, \quad 0 < G, B < 1. \quad (10)$$

Equation (10) defines a polaron function $|\Psi_K(G, B)\rangle$ which is completely determined by two parameters, G and B .

In what follows, two different approaches are presented. The first, denoted by the index T (T for translational), treats G and B as the variational parameters for which the energy minimum E_T has to be found, and its corresponding polaron function is $|\Psi_K^T\rangle$. The T method gives good results in the weak- and the strong-coupling regime. Namely, in both of these limits, the function $|\Psi_K^T\rangle$ becomes similar to the polaron function obtained by the appropriate perturbative calculations.

In the second approach, the variational method is used to define a generalized eigenvalue problem as follows. The polaron wave function, denoted by the index CT (CT for com-

bination of translational functions), is rewritten as a linear combination of functions $|\Psi_K(G_n, B_n)\rangle$,

$$|\Phi_K^{CT}\rangle = \sum_{n=1}^p a_n |\Psi_K(G_n, B_n)\rangle. \quad (11)$$

It is understood here that the functions $|\Psi(G_n, B_n)\rangle$ form a set of p generally nonorthogonal functions, defined by p different pairs of parameters (G_n, B_n) . Again, the coefficients a_n should be determined from the requirement that the expectation value of the energy,

$$\bar{E}_{CT} = \frac{\langle \Phi_K^{CT} | \hat{H} | \Phi_K^{CT} \rangle}{\langle \Phi_K^{CT} | \Phi_K^{CT} \rangle},$$

is minimal,

$$\partial \bar{E}_{CT} / \partial a_n^* = 0, \quad 1 \leq n \leq p,$$

or,

$$\begin{aligned} \sum_{n'} \langle \Psi_K(G_n, B_n) | \hat{H} | \Psi_K(G_{n'}, B_{n'}) \rangle a_{n'} \\ = E_{CT} \sum_{n'} \langle \Psi_K(G_n, B_n) | \Psi_K(G_{n'}, B_{n'}) \rangle a_{n'}. \end{aligned}$$

The solution of this generalized eigenvalue problem is a set of p orthogonal polaron functions, $|\Phi_{K,m}^{CT}\rangle$, with corresponding energies $E_{CT}^{(m)}$. The ground-state energy is $E_{CT}^{(0)}$. One may always include the function $|\Psi_K^{(0)}\rangle$ in the sum (11) in order to ensure that the energy $E_{CT}^{(0)}$ is the same or better than E_T , the energy computed by the T method. Moreover, by paying further attention to the starting set of functions $|\Psi_K(G_n, B_n)\rangle$ in Eq. (11) at the outset, one is able to investigate the first excited state $|\Phi_{K,m=1}^{CT}\rangle$ of the system, when this state corresponds to an excited polaron. The best results for the CT method are obtained when the number p of $|\Psi_K(G_n, B_n)\rangle$ functions in Eq. (8) changes with the Hamiltonian parameters. The special case where the CT method is used with constant $p=2$ is denoted by the index CT^2 .

C. eT and eL methods:

Exact translational and exact localized polaron functions

Finally, this paper presents the results of two numerical exact diagonalization methods.^{19–23} In order to compute the low-energy polaron states, one approximates the infinite dimensional Hamiltonian matrix with a finite one, and proceeds with the exact diagonalization of this matrix. The lowest eigenvalue and eigenvector in such a reduced Hilbert space correspond to the polaron energy and wave function, respectively. For a large sparse matrix, the energy and the wave function can be calculated very accurately, by using an appropriate numerical scheme, in the present case the Lanczos algorithm.

The two exact diagonalization methods used here differ in the choice of the basis of the Hilbert space. In the first

method,²³ denoted by eT (e stands for exact diagonalization and T for translational), the general orthonormal state is given by

$$\begin{aligned} |n_0, n_{-1}, n_1, \dots, n_m, \dots\rangle_K^{eT} \\ = \frac{1}{\sqrt{N}} \sum_j e^{iKja} c_j^\dagger |n_0, n_{-1}, n_1, \dots, n_m, \dots\rangle_j, \end{aligned} \quad (12)$$

which describes an eigenstate of the system with momentum K . n_m is the number of phonons at the m th lattice site away from the electron. For example, at the site j , and at the nearest-neighbor lattice sites left and right from it, there are n_0 , n_{-1} , and n_1 phonons, respectively. The Hamiltonian (1) does not mix states (12) with different momenta. Therefore the polaron function obtained by the eT method has the same K momentum as the basis states. The current implementation of the eT method is highly accurate, and from a practical point of view may be treated as exact.²³ For this reason, the eT results can be used to determine the numerical errors present in the other methods.

The minimal number of states of the reduced basis necessary to obtain accurate results depends on the Hamiltonian parameters. This number for the eT method increases very rapidly for $\hbar\omega \ll g, t$, which prevents its use for both large g and t .

In the second exact diagonalization method, denoted by eL (e stands for exact diagonalization and L for localized), the general orthonormal state of the chosen basis is more complicated than for the eT method,

$$\begin{aligned} |i, n_0, n_{-1}, n_1, \dots, n_m, \dots; \xi_m\rangle_j^{eL} \\ = c_{j+i}^\dagger \left(\prod_m S_{j+m}(\xi_m) \right) |n_0, n_{-1}, n_1, \dots, n_m, \dots\rangle_j. \end{aligned} \quad (13)$$

Here the i and m indices are given with respect to the center of polaron, which is placed at the site j . Thus c_{j+i}^\dagger creates an electron at the i th site from the polaron center at j , n_m is the number of extra phonons at the m th site away from the polaron center, when the lattice is already distorted by the coherent state operators $S_{j+m}(\xi_m)$, i.e., $\bar{x}_{j+m} = 2x_0\xi_m$. The eL method calculates localized polaron wave functions. Namely, Eq. (13) describes a localized state, with the polaron center at site j kept constant. The eL method is therefore accurate only in the strong-coupling regime, in which the effects of polaron delocalization are negligible (self-trapped polarons).

For a given set of Hamiltonian parameters, ξ_m in Eq. (13) are determined by the use of the L method, i.e., by minimizing the energy (5), $\xi_m = \xi_m^L$. If only those states (13) with all $n_m=0$ are used in calculations, the eL method gives the same polaron wave function as the L method. The additional states (13), with n_m phonon excitations, are necessary to obtain the actual equilibrium positions of the lattice in the exact localized polaron state and the zero-point motion of the renormalized lattice vibrations. It is worth noting that the

electron and phonon parts of the eL polaron wave function cannot be completely separated, as in the case of the L function.

In the case of eL method, the mean lattice deformation of the localized polaron is approximately taken care of by the product of the coherent states operators, $\Pi_m S_{j+m}(\xi_m)$, which keeps the necessary number of states (13), in the eL method, relatively small. In order to reduce the basis of the Hilbert space, the maximal allowed distance of the electron and phonons from the polaron center has been limited here by the choice $|i|, |m| \leq D^{max}$. The distance D^{max} has been determined from the condition that $\xi_m/\xi_0 < 10^{-4}$ if $m > D^{max}$. The maximal total number of phonons has been kept limited, retaining the states with $\sum_m n_m \leq 4$. As the sum $\sum_m n_m$ does not include the phonons associated with the coherent state operators $S_{j+m}(\xi_m)$, the small value of $\sum_m n_m$ is not a restriction on the overall amplitude of the lattice deformation. The accuracy of the results obtained by the eL method, supplemented by the two above-mentioned criteria, depends of course on the values of parameters.

For the purpose of clarity, it seems appropriate at this point to review briefly the notation L , T , CT , eT , and eL of all five presented methods. All methods based on the localized polaron function are denoted by the letter L (L and eL methods), whereas all methods based on the translational function are denoted by the letter T (T , CT , and eT methods). The letter e denotes an exact diagonalization method (eT and eL methods), while a single letter notation (L and T) suggests the simplest form of the method.

IV. RESULTS

As the variational methods of the preceding section themselves, the results of the corresponding calculations may be best understood in terms of the weak- and strong-coupling limits and the crossover between them. It has been shown previously,²⁴ on the basis of the global-local method for $0.1\hbar\omega < t < 10\hbar\omega$, that the empirical relation

$$g_{ST} = \hbar\omega + \sqrt{t\hbar\omega} \quad (14)$$

describes well the values of parameters for which the variation of the effective polaron mass with g is the fastest. It will be also argued here that g_{ST} of Eq. (14) describes accurately the crossover from the weak- to the strong-coupling limit with respect to the nature of the $K=0$ ground state. The latter changes continuously from the light delocalized state in the weak-coupling limit to the heavy self-trapped state in the strong-coupling limit, with the anticrossing of the two states at $g \approx g_{ST}$. The physical content of Eq. (14) is best understood by considering the limits of small and large t with respect to $\hbar\omega$, when, respectively, $g_{ST} \approx \hbar\omega$ and $\varepsilon_p^{ST} = g_{ST}^2/\hbar\omega \approx t$. Both these conditions were qualitatively explained in Ref. 25. In the present section we first discuss the strong- and the weak-coupling limit, and then devote most of our attention to the crossover between the two.

A. Strong-coupling limit

The nature of the self-trapped polaron may be discussed by analyzing the properties of the two polaron wave func-

tions given by Eqs. (4) and (8). When the localized polaron functions $|\varphi_j\rangle$ at different lattice sites are not orthogonal,

$$S_\Delta = \langle \varphi_j | \varphi_{j+\Delta} \rangle \neq \delta_{0,\Delta},$$

the local properties and delocalization effects of $|\Psi_K\rangle$ in Eq. (8) are a complex mixture. However, in both the weak- and strong-coupling regimes, the translational polaron function can be approximately written in terms of orthogonal localized polaron functions. In the weak coupling regime, the orthogonality follows from the electron part of the wave function,

$$S_\Delta \sim \sum_n \eta_n^* \eta_{n+\Delta} \approx \delta_{0,\Delta},$$

while in the strong-coupling regime, it follows from the lattice part,

$$S_\Delta \sim Y_\Delta = \exp\left(-\frac{1}{2} \sum_m (\xi_m^* - \xi_{m+\Delta})^2\right) \approx \delta_{0,\Delta}. \quad (15)$$

In Eq. (15), Y_Δ is the Debye-Waller factor. The condition (15) corresponds to the regime of self-trapped polarons. The negligible contribution of the lattice part to the overlap of any two localized polaron functions at different lattice sites results then in a negligible polaron hopping energy t_{pol} .

One may notice that in the limit $Y_{\Delta \neq 0} \rightarrow 0$ the translational form of the polaron function (8) has no consequences on polaron energy, and the minimal values of the variational energies (5) and (9) coincide, i.e., E_Δ , $S_\Delta \sim \delta_{0,\Delta}$ in Eq. (9). The hopping of the self-trapped polaron occurs only at the time scale which is much larger than the scale relevant for the local interplay between the electron and the lattice deformation. Therefore an accurate description of the local polaron properties may be obtained even if the hopping of the polaron is completely omitted by using only localized polaron functions. The translational invariance of the polaron may be, however, always restored in the same way as the function (4) is used to obtain Eq. (8).

The eL method provides very accurate results for the ground-state energy of the self-trapped polaron. Except that it neglects the polaron hopping, the local polaron function is calculated exactly. The error of the eL method may be estimated by using the eT method, that is, by subtracting the exact energy of zero-momentum polaron state E_{eT} from E_{eL} . For the electron-phonon coupling which is greater than the critical electron-phonon coupling in Eq. (14) just by $\hbar\omega$, i.e., $g = g_{ST} + \hbar\omega$, the maximal error of the eL method is $E_{eL} - E_{eT} < 3 \times 10^{-4} \hbar\omega$. This is shown in Fig. 1, in which two qualitative estimates of t_{pol} in the strong-coupling regime are plotted as well. The first estimate gives t_{pol} as one-fourth of the polaron bandwidth computed exactly by the eT method,

$$t_{pol} \sim \frac{1}{4} W^{eT} = \frac{1}{4} [E_{eT}(K = \pi/a) - E_{eT}(K = 0)], \quad (16)$$

while the second estimate, based on the L method, multiplies the electron hopping energy with the small Debye-Waller factor,

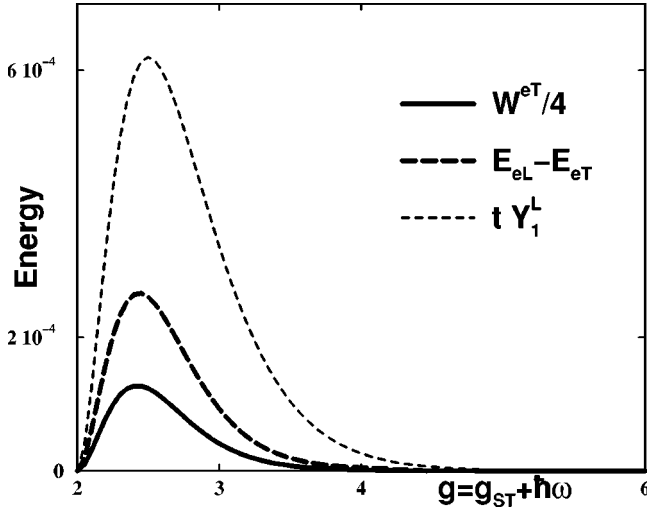


FIG. 1. The solid curve is one-fourth of the polaron bandwidth, Eq. (16). The long-dashed curve corresponds to the error of the polaron energy calculated by the eL method, $E_{eL} - E_{eT}$. The short-dashed curve is the electron hopping energy reduced by the Debye-Waller factor, Eq. (17). All three curves are given as functions of the electron-phonon coupling $g = g_{ST} + \hbar\omega = \sqrt{t\hbar\omega} + 2\hbar\omega$. The energies are given in units of $\hbar\omega$ (i.e., $\hbar\omega = 1$).

$$t_{pol} \sim t Y_1^L = t \exp\left(-\frac{1}{2} \sum_m (\xi_m^L - \xi_{m+1}^L)^2\right). \quad (17)$$

The estimation of the Debye-Waller factor in Eq. (17) is based on the evaluation of the lattice part of the overlap of the two neighboring $|\varphi_j^L\rangle$ functions (the L method gives good results for the mean lattice deformation of the self-trapped polarons). All three curves in Fig. 1 are similar functions of g , which is not surprising since all plotted quantities are related to the polaron hopping energy t_{pol} in the strong-coupling regime. Moreover, it may be seen from Fig. 1 that the error of the eL method is almost equal to one-half of the polaron bandwidth,

$$E_{eL} - E_{eT} \approx W^{eT}/2.$$

One of the advantages of the eL method is that it permits separate calculations of the electron and the lattice properties, in spite of the fact that the electron and the phonon part of the eL wave function are not separable. For instance, for the polaron centered at the origin, the associated mean lattice deformation \bar{x}_n is given simply by the expectation value of \hat{x}_n of Eq. (2). Besides \bar{x}_n , in the present paper the mean real space uncertainty of the on-site lattice vibration $\overline{\Delta x_n}$ and the product $\overline{\Delta x_n \Delta p_n}$, where $\overline{\Delta p_n}$ is the mean momentum uncertainty of the on-site lattice vibration, are calculated.

Figure 2 shows the data for two sets of parameter, corresponding to a small self-trapped polaron and a self-trapped polaron extended over few lattice sites, respectively. For the second set of parameter (large g and t), the eT method is not accurate enough, and the question arises of whether the eL polaron state is really a good approximation of the system ground state. It is difficult to prove that a polaron state, with non-negligible hopping energy t_{pol} and an energy close or lower than eL energy, does not exist. This question is currently under investigation.

Differences between the results of the L and the eL methods are also analyzed. It is found that they are more pronounced for small g . We may see from the results in Fig. 2 that the mean lattice deformation differs between these two methods. In the case of the eL method, the mean lattice deformation is more extended and the width of the polaron is slightly larger. Additionally, the electron density of the eL method remains approximately proportional to the mean lattice deformation [as in Eq. (6), valid for the L method], since

$$\left(x_n^{eL} - \frac{2g}{\hbar\omega} \varrho_n^{eL} x_0\right) / x_n^{eL} < 1\%.$$

As has already been mentioned, the lattice part of the L function describes a set of displaced, but unrenormalized, harmonic oscillators, so $\Delta x_n^L = x_0$, $\Delta p_n^L = p_0$, where x_0 and p_0

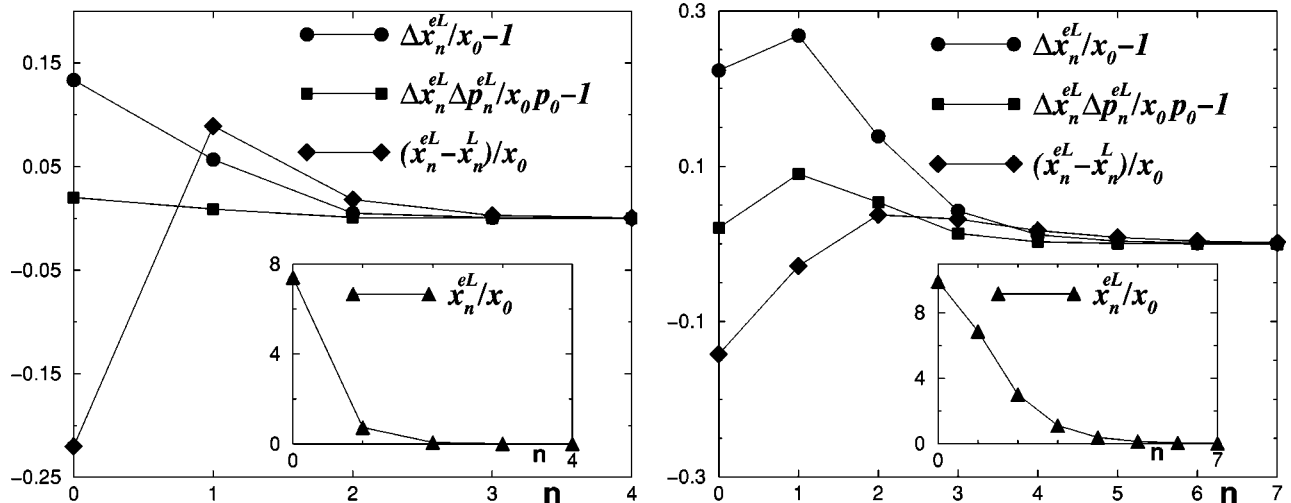


FIG. 2. Difference between the mean lattice deformation, mean uncertainty of the on-site lattice vibration and corresponding product of uncertainties for the L and eL methods. The inset shows the mean lattice deformation of the eL method. Hamiltonian parameters are $t = 10\hbar\omega$, $g = 4.5\hbar\omega$, and $t = 250\hbar\omega$, $g = 16.5\hbar\omega$, for the first and second plot, respectively.

are defined in Eq. (2). One may notice from Fig. 2 that real-space uncertainties of the lattice vibrations on the sites occupied by the polaron are larger in the eL case than in the L case, $\Delta x_n^{eL} > x_0$, but uncertainties of on-site momentum lattice vibrations are smaller, $\Delta p_n^{eL} < p_0$.

It may be concluded, from the first plot in Fig. 2 that the electron affects mostly the central site of the small polaron. The product of uncertainties for this site stays close to the free lattice value, $\Delta x_{n=0}^{eL} \Delta p_{n=0}^{eL} \approx x_0 p_0$. Therefore the phonon mode at the central site of the small polaron may be treated, in a good approximation, as harmonic. In particular, the renormalized frequency of this mode, $\tilde{\omega}_{n=0}^{eL}$, can be roughly estimated from the relation

$$\Delta x_{n=0}^{eL} \approx \sqrt{\hbar/2M\tilde{\omega}_{n=0}^{eL}}.$$

Since $\Delta x_{n=0}^{eL} > x_0$, it follows that $\tilde{\omega}_{n=0}^{eL} < \omega$. Therefore in the strong-coupling regime the first excited state should correspond to the excitation of the renormalized phonon mode, rather than to the excitation of the phonon of energy $\hbar\omega$, which is uncorrelated to the polaron. One may also notice that the energy of the mean lattice deformation is larger for the eL method than the L method (for the L method this energy is minimal). This is compensated for, however, with the lower energy associated with the zero-point motion of the $\tilde{\omega}_{n=0}^{eL}$ phonon mode, which makes the total polaron energy of the eL method lower.

For the more extended self-trapped polarons, the renormalized normal phonon modes are expected to be spread over a number of lattice sites. Consequently, a number of different phonon modes contribute to the lattice displacement at the lattice sites occupied by the polaron. Thus the analysis of the on-site vibrations cannot give direct information on the renormalized lattice modes. Nevertheless, from the second plot in Fig. 2 one may notice that the product of uncertainties $\Delta x_n^{eL} \Delta p_n^{eL}$ shows a minor deviation from that of the harmonic vibration. This suggests that the renormalized lattice modes of the extended self-trapped polaron are harmonic as well in a good approximation.

B. Weak-coupling regime

In the weak-coupling regime, the T method gives results close to the eT results. Since the form of the function T is quite simple, it will be used in this section as a basis for further discussion. In the weak-coupling regime, the minimum of the variational energy E_T corresponds to small values of the variational parameters G and A . The standard perturbative ground state of the system with momentum K in terms of the T method polaron function may be written as follows:

$$|\Psi_K^T\rangle = \frac{1}{\sqrt{N_\Psi}} \sum_j e^{iKja} c_j^\dagger \times \left(1 + A \sum_m B^{|m|} e^{iKma} b_{j+m}^\dagger \right) |0\rangle, \quad K < K_c, \quad (18)$$

$$b_k^\dagger |\Psi_{K=0}^T\rangle = b_k^\dagger \frac{1}{\sqrt{N_\Psi}} \sum_j c_j^\dagger \left(1 + A \sum_m B^{|m|} b_{j+m}^\dagger \right) |0\rangle, \quad K > K_c. \quad (19)$$

For $K < K_c$ the wave function (18) has two parts. The main part corresponds to the free electron of momentum K , and the smaller part, proportional to A , corresponds to the electron dressed by one spatially correlated virtual phonon. At the threshold K_c , the energy of such a polaron state intersects with the energy of the system consisting of the zero-momentum polaron and one extra phonon with momentum K_c , Eq. (19). So, for $K > K_c$ the ground state is achieved with one real phonon in the system which carries the system momentum and which is spatially uncorrelated with the polaron.^{13,26} For $K < K_c$ this state becomes the first excited state of the system. The difference between the energies of the ground state and the first excited state is the largest for $K=0$, and is equal to $\hbar\omega$.

The validity of the perturbative treatment requires that the weight of the second term in Eqs. (18) and (19) is small, i.e., the mean number of phonons associated with the lattice deformation has to satisfy

$$\bar{N}_{ph}^{pol} = A^2(1+B^2)/(1-B^2) = \frac{g^2}{(\hbar\omega)^2} \frac{(1-B)(1+B^2)}{(1+B)^3} \ll 1. \quad (20)$$

Here, A has been eliminated by using Eq. (3). There are two ways to satisfy condition (20). Either the electron-phonon coupling is small, $g \ll \hbar\omega$, or the lattice deformation is spread to a large number of lattice sites, $1-B \ll 1$. In the latter case, the total mean polaron deformation does not have to be small, $\bar{x}_{tot}/x_0 = 2g/\hbar\omega$, since g can be larger than $\hbar\omega$.

The translationally invariant form of the wave function for the T method, given by Eq. (8), provides an energy gain due to the polaron delocalization. At the same time, the spatial correlation between the electron and the lattice deformation has a finite length. For instance, in Eq. (8), this length is of the same order for $|\Psi_K\rangle$ and $|\varphi_j\rangle$. The perturbative calculation for B in Eq. (18) gives

$$B = \cos(Ka) + \hbar\omega/2t - \sqrt{[\cos(Ka) + \hbar\omega/2t]^2 - 1}.$$

B measures the electron-lattice correlation length. B is independent of g , which makes the correlation length finite, even in the limit $g \rightarrow 0$ for which the lattice deformation vanishes, $A \sim g/\hbar\omega$.

On the other hand, the electron-lattice deformation correlation length and the polaron delocalization range are of the same order for the localized functions. This may be easily seen from Eq. (4). In the limit $g \rightarrow 0$ they both become infinite. Thus in the weak-coupling regime one obtains a localized polaron state $|\varphi_j^L\rangle$ of very large width, but associated with a tiny lattice deformation. This is specific for one-dimensional systems in which an attractive symmetric potential has always a bound electron state. Therefore the corresponding polaron energy is less than the free electron energy $-2t$. In higher dimensions, an arbitrary attractive symmetric

potential does not have a bound electron state for sufficiently small g (or the electron binding energy is too small to balance the lattice deformation energy), and the total polaron energy is larger than $-2dt$, where d is the dimension of the system. This explains why, in the weak-coupling regime, the adiabatic (localized) polaron functions^{11,27,28} fail to have an energy lower than the free-electron energy, for the dimension of the system greater than 1. A detailed parallel perturbative analysis of polarons in one, two, and three dimensions is given in Ref. 29.

C. Crossover regime

In the crossover regime the polaron hopping energy t_{pol} is not negligible, and the translationally invariant polaron functions should be used in order to obtain the full physical picture of the polaron. In order to calculate the numerical errors of different methods accurately, the present discussion of the crossover regime is restricted to the values of t smaller than $25\hbar\omega$, for which results from the eT method are available.

In order to examine the crossover regime it is instructive to calculate the energy difference between the ground and first excited state, $E_{CT}^{(1)} - E_{CT}^{(0)}$. Let g_c denote the value of g for which this difference is minimal,

$$\partial(E_{CT}^{(1)} - E_{CT}^{(0)})/\partial g|_{g=g_c} = 0.$$

Our results indicate that g_c is very close to the value of g_{ST} given by Eq. (14). For example, for $t = 20\hbar\omega$, $g_c = 5.55\hbar\omega$, while $g_{ST} = 5.47\hbar\omega$. For smaller t , g_c and g_{ST} coincide even better. The analysis of the effective mass,²⁴ variational energy of the polaron ground state,³⁰ polaron size,³¹ as well as the behavior of the first excitation energy, suggest that a dramatic change in the nature of the polaron ground state and the first excited state are intimately related in the crossover regime.

This can be well understood by considering the properties of the wave function in the T method. Near g_c , this polaron wave function has two separate energy minima in the G - B parameter space defined by Eq. (10), which become degenerate for $g = g_c$. Let the symbol $<$ denote the lower minimum at $g < g_c$, and the symbol $>$ the lower minimum at $g > g_c$. $|\Psi^< \rangle$ and $|\Psi^> \rangle$ are the corresponding polaron wave functions. Even if they are not mutually orthogonal, they are still physically quite different. The numerical data show that the translational invariance of $|\Psi^< \rangle$ contributes strongly to the polaron energy. On the other hand, the translational invariance of $|\Psi^> \rangle$ has almost negligible energy contributions, i.e., $|\Psi^> \rangle$ describes an almost self-trapped polaron. It is worth noting that the degenerate nature of the variational energy which has been reported for the Toyozawa method¹³ is of the same kind as the one of the T method discussed here. Namely, both T and Toyozawa method are based on the same polaron function (8).

$|\Psi^< \rangle$ and $|\Psi^> \rangle$ can be combined to form new polaron functions,

$$|\Phi^{CT^2}\rangle = a_<|\Psi^< \rangle + a_>|\Psi^> \rangle. \quad (21)$$

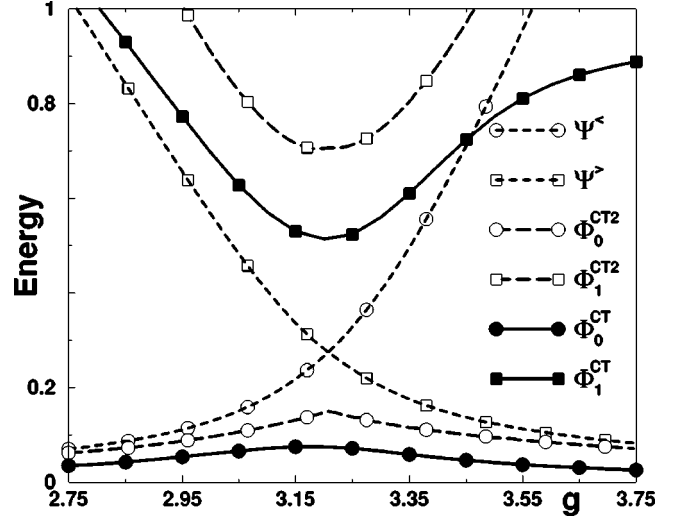


FIG. 3. The anticrossing of $|\Psi^< \rangle$ and $|\Psi^> \rangle$ energies together with the ground state $|\Phi_0^{CT^2}\rangle$ and first excited state $|\Phi_1^{CT^2}\rangle$ energies are shown. The results of the CT method are also plotted for comparison. The ground-state energy obtained by the eT method is subtracted from all energy curves. $t = 5\hbar\omega$, $K = 0$, and $\hbar\omega = 1$, while $g_{ST} = 3.24\hbar\omega$.

It should be mentioned that a similar combination of two states has been already used in Ref. 32 in order to calculate the polaron ground state. $|\Phi^{CT^2}\rangle$ corresponds to Eq. (11) with $p = 2$, which means that the CT^2 method is implied. From this treatment the improved ground state $|\Phi_0^{CT^2}\rangle$ and the approximate first excited polaron state $|\Phi_1^{CT^2}\rangle$ are obtained. It may be seen from Fig. 3 that CT^2 method describes an anticrossing of $|\Psi^> \rangle$ and $|\Psi^< \rangle$ states, which yields two orthogonal states, $|\Phi_0^{CT^2}\rangle$ and $|\Phi_1^{CT^2}\rangle$. In order to have a better illustration of that anticrossing in Fig. 3, the exact ground-state energy E_{eT} is subtracted from all plotted energy curves. For $g < g_c$ the *light* state $|\Psi^< \rangle$ is lower in energy, and participates in the ground state more than the *heavy* state $|\Psi^> \rangle$. However, as g increases this balance changes continuously in favor of $|\Psi^> \rangle$. The opposite trend is observed for the first excited state, which is heavier than the ground state for smaller g and lighter for larger g .

The CT method gives better results for the ground and first excited state when a large number of functions (large p) in Eq. (11) is used. From Fig. 3, one may estimate that $E_{CT}^{(1)} - E_{CT}^{(0)} \approx \hbar\omega/2$ at $g = g_c$. Moreover, the energy $E_{CT}^{(1)}$, unlike $E_{CT^2}^{(1)}$, satisfies $E_{CT}^{(1)} < E^{(0)} + \hbar\omega$ for all $g > g_c$, which is an important improvement over the $p = 2$ result.

V. SUMMARY OF RESULTS

Figure 4 shows the results for the ground-state energy and the energy of the first excited state with total system momentum $K = 0$, as functions of g , obtained by several different methods. Two plots correspond to $t = 5\hbar\omega$ and $t = 10\hbar\omega$, respectively. The ground-state energy obtained by the eT method is subtracted from all the other results. g_1 and g_2 are used to mark three different polaron regimes with respect to

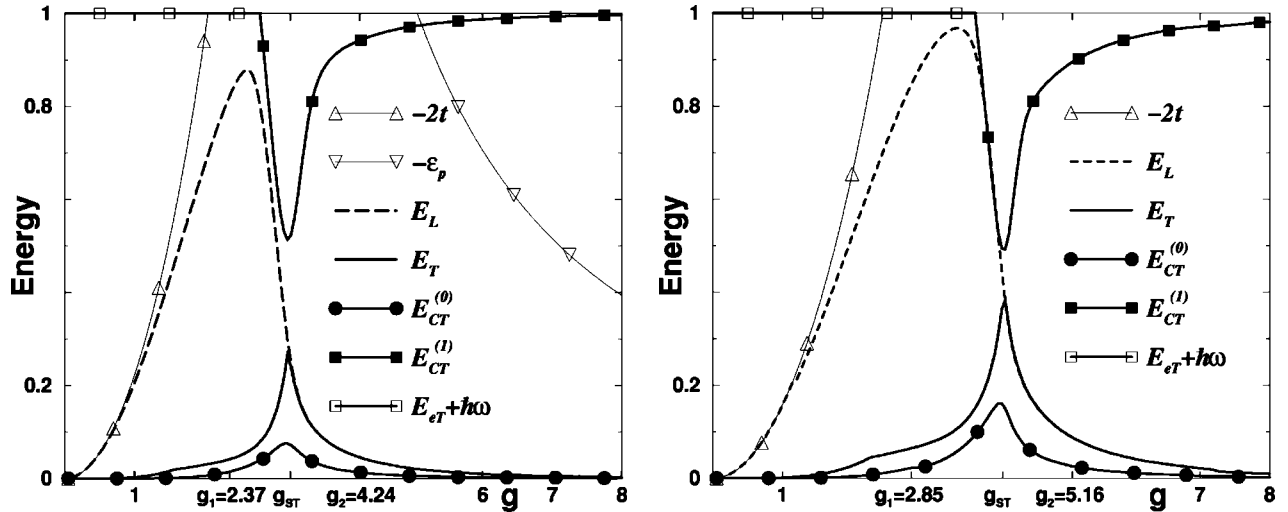


FIG. 4. The ground-state energy of the polaron for various methods and the first excited-state energy of the CT method are plotted for $t=5\hbar\omega$ and $t=10\hbar\omega$, respectively. $K=0$ and $\hbar\omega=1$ for both plots. The eT ground-state energy is subtracted from all results. Only the lowest $\hbar\omega$ energy interval of the spectrum, relevant for the ground and first excited energy, is shown. The $E_{eT}+\hbar\omega$ line denotes the first excited-state energy, when it consists of the polaron ground state and one extra phonon; see Eq. (19).

the strength of the electron-phonon coupling. For $g < g_1$ the mean number of phonons of the lattice deformation is less than 1. Thus for $g \lesssim g_1$ we recognize the weak-coupling regime. For $g > g_2 = g_{ST} + \hbar\omega$ the eL polaron energy has a negligible error (see Fig. 1), which means that for $g \gtrsim g_2$ polarons are self-trapped, and we recognize the strong-coupling regime. The crossover regime is found in the interval $g_1 \lesssim g \lesssim g_2$, with $g_1 < g_{ST} \approx g_c < g_2$.

It may be noted from Fig. 4 that in the weak-coupling regime, the energy obtained by the L method (E_L) is close to the free-electron energy $-2t$ (for $t \gtrsim 20\hbar\omega$, the absolute error of the L method becomes greater than $\hbar\omega$ in some intervals of g). In the strong-coupling regime, for large g , E_L approaches the exact polaron energy.

The error of the T method, as may be seen from Fig. 4, is the largest in the crossover regime in which the results can be improved by a better choice of η_n and ξ_m in Eq. (10). In the strong-coupling regime, the translationally invariant form of the function T has no effect on the polaron energy, i.e., both the T and L methods give very similar results.

The energy of the first excited polaron state, $E_{CT}^{(1)}$, intersects the energy of the ground state plus one phonon, $E_{eT} + \hbar\omega$, for $g > g_1$. After the minimum of $E_{CT}^{(1)} - E_{CT}^{(0)}$ is reached in the crossover regime at $g = g_c \approx g_{ST}$, $E_{CT}^{(1)}$ approaches $E_{eT} + \hbar\omega$ asymptotically for $g > g_2$. As has already been pointed out in Sec. IV, the excitation of the renormalized phonon mode explains the nature of the first excited state in the strong-coupling limit. In Ref. 28 perturbation theory was used to calculate the frequency of this local phonon mode, $\tilde{\omega}'$, to the lowest order in $t\hbar\omega/g^2$,

$$\tilde{\omega}' = \omega \sqrt{1 - (t\hbar\omega/g^2)^2}. \quad (22)$$

The obtained perturbative correction to the phonon frequency is adiabatic, i.e., the square root in Eq. (22) is independent of mass M . It is worth noting that for large g , $E_{CT}^{(1)}$

calculated here shows approximately the same behavior as the energy of the ground state with one additional phonon of frequency (22),

$$E_{CT}^{(1)} \approx E_{eT} + \hbar\tilde{\omega}'.$$

The lattice part of the CT function is spatially symmetric with respect to the electron. Therefore in the strong-coupling regime the first excited state, which has been identified here as a local renormalized phonon mode of the self-trapped polaron, should be basically a symmetric oscillation of the lattice deformation around the central polaron site. In the vicinity of g_{ST} , on the other hand, the nature of the first excited state is currently explained by the anticrossing of the self-trapped and the delocalized polaron state. The question of how the excited self-trapped polaron state in the strong-coupling regime and the first excited state near g_{ST} may be linked together is a matter of further considerations. One may speculate that the anticrossing of the excited self-trapped polaron state and the delocalized state will give the answer.

VI. CONCLUSIONS

The present paper discusses the ground and first excited states of the polaron for three different regimes of the electron-phonon coupling parameter g . The results can be briefly summarized as follows. In the strong-coupling regime the polaron hopping energy to neighboring sites is negligible, and the self-trapped polaron states are obtained. The results of the eL method suggest that the adiabatic picture of the localized polaron state is valid, in which some of the local lattice vibrations are renormalized by the presence of the electron. The numerical data show no significant deviation from the adiabatic locking relation (6) of the electron site density and the mean lattice deformation. In the small polaron case, the predominant effect of the electron is the low-

ering of the frequency of the vibration at the central polaron site. The excitation of the renormalized phonon mode corresponds to the first excited state of the small self-trapped polaron.

The nature of the polaron ground state in the crossover regime has been discussed in a number of papers, and its rapid change with g has been well established numerically. The difference between the energies of the first excited state and the ground state, as a function of g , has a minimum for $g = g_c$. It is shown, by using the CT^2 method, that the anti-crossing of the self-trapped and the delocalized polaron state can link the behavior of the ground and first excited polaron state. According to the CT method, for $g > g_c$ the effective mass of the ground state is larger than the effective mass of the first excited state, while for $g < g_c$ the opposite is true. In addition, it is found that g_c , which characterizes the first excited state, and g_{ST} , obtained from ground state analysis [Eq. (14)] almost coincide for $t < 25\hbar\omega$.

Upon further reduction of g the total mean number of phonons bound by the polaron becomes smaller than 1, and the weak-coupling regime is reached. The nearly free electron is dressed by a cloud of virtual phonons, and its mass is slightly renormalized. The first excited state of the system, with momentum $K \approx 0$, can be viewed as the ground state of the polaron plus one additional uncorrelated phonon, rather than as an excited polaron.

Finally, it is worth noting that there is a simple sum rule

for the mean total lattice deformation, Eq. (3), which is valid for any number of electrons and is independent of the system dimension. This important sum rule may be extended to some other models in which the lattice deformation is linearly coupled to the local electron density.

ACKNOWLEDGMENTS

The author would like to thank I. Batistić for fruitful collaboration during the course of this work.

APPENDIX

In order to calculate S_Δ and E_Δ of Eq. (9), the following expressions may be used:

$$Y_\Delta = \exp\left(-\frac{1}{2} \sum_m (\xi_m^* - \xi_{m+\Delta})^2\right),$$

$$S_\Delta = Y_\Delta \sum_n \eta_n^* \eta_{n+\Delta},$$

$$E_\Delta = -tY_\Delta \sum_n \eta_n^* (\eta_{n+\Delta+1} + \eta_{n+\Delta-1}) + \hbar\omega S_\Delta \sum_m \xi_m^* \xi_{m+\Delta} - gY_\Delta \sum_n \eta_n^* \eta_{n+\Delta} (\xi_n^* + \xi_{n+\Delta}).$$

*Electronic address: obaristic@ifs.hr

¹L. D. Landau, *Z. Phys.* **3**, 644 (1933).

²T. Holstein, *Ann. Phys. (N.Y.)* **8**, 325 (1959).

³H. De Raedt and A. Lagendijk, *Phys. Rev. Lett.* **49**, 1522 (1982); *Phys. Rev. B* **27**, 6097 (1983); **30**, 1671 (1984).

⁴P. E. Kornilovitch and E. R. Pike, *Phys. Rev. B* **55**, R8634 (1997).

⁵D. W. Brown, K. Lindenberg, and Y. Zhao, *J. Chem. Phys.* **107**, 3179 (1997).

⁶C. Zhang, E. Jeckelmann, and S. R. White, *Phys. Rev. Lett.* **80**, 2661 (1998); *Phys. Rev. B* **60**, 14 092 (1999); E. Jeckelmann and S. R. White, *ibid.* **57**, 6376 (1998).

⁷P. Gosar, *J. Phys. C* **8**, 3584 (1975).

⁸A. S. Alexandrov, *Phys. Rev. B* **61**, 12 315 (2000).

⁹B. Gerlach and H. Löwen, *Phys. Rev. B* **35**, 4291 (1987); *Rev. Mod. Phys.* **63**, 63 (1991); H. Löwen, *Phys. Rev. B* **37**, 8661 (1988).

¹⁰D. Feinberg, S. Ciuchi, and F. de Pasquale, *Int. J. Mod. Phys. B* **4**, 1395 (1990).

¹¹G. Kalosakas, S. Aubry, and G. P. Tsironis, *Phys. Rev. B* **58**, 3094 (1998).

¹²Y. Toyozawa, *Prog. Theor. Phys.* **26**, 29 (1961).

¹³Y. Zhao, D. W. Brown, and K. Lindenberg, *J. Chem. Phys.* **107**, 3159 (1997).

¹⁴H. B. Shore and L. M. Sander, *Phys. Rev. B* **7**, 4573 (1973).

¹⁵K. H. Hock, H. Nickisch, and H. Thomas, *Helv. Phys. Acta* **56**, 237 (1983).

¹⁶G. Venzl and S. F. Fischer, *Phys. Rev. B* **32**, 6437 (1985).

¹⁷A. Klamt, *J. Phys. C* **21**, 1953 (1988).

¹⁸A. La Magna and R. Pucci, *Phys. Rev. B* **53**, 8449 (1996).

¹⁹J. Ranninger and U. Thibblin, *Phys. Rev. B* **45**, 7730 (1992).

²⁰F. Marsiglio, *Phys. Lett. A* **180**, 280 (1993); *Physica C* **244**, 21 (1995).

²¹A. S. Alexandrov, V. V. Kabanov, and D. K. Ray, *Phys. Rev. B* **49**, 9915 (1994).

²²G. Wellein and H. Fehske, *Phys. Rev. B* **56**, 4513 (1997); **58**, 6208 (1998).

²³J. Bonča, S. A. Trugman, and I. Batistić, *Phys. Rev. B* **60**, 1633 (1999).

²⁴A. H. Romero, D. W. Brown, and K. Lindenberg, *Phys. Rev. B* **59**, 13 728 (1999).

²⁵M. Capone, W. Stephan, and M. Grilli, *Phys. Rev. B* **56**, 4484 (1997).

²⁶J. M. Robin, *Phys. Rev. B* **58**, 14 335 (1998).

²⁷D. Emin and T. Holstein, *Phys. Rev. Lett.* **36**, 323 (1976).

²⁸V. V. Kabanov and O. Yu. Mashtakov, *Phys. Rev. B* **47**, 6060 (1993).

²⁹A. H. Romero, D. W. Brown, and K. Lindenberg, *Phys. Lett. A* **254**, 287 (1999).

³⁰A. H. Romero, D. W. Brown, and K. Lindenberg, *Phys. Rev. B* **60**, 4618 (1999).

³¹A. H. Romero, D. W. Brown, and K. Lindenberg, *Phys. Lett. A* **266**, 414 (2000).

³²V. Cataudella, G. De Filippis, and G. Iadonisi, *Phys. Rev. B* **60**, 15 163 (1999); **62**, 1496 (2000).